Available online at www.sciencedirect.com
ScienceDirect
Bioelectrochemistry 71 (2007) 81–90
Bioelectrochemistry
www.elsevier.com/locate/bioelechem

Parallel synthesis of libraries of anodic and cathodic functionalized electrodeposition paints as immobilization matrix for amperometric biosensors

Bertrand Ngounou [a], Elchin H. Aliyev [b], Dmitrii A. Guschin [a], Yusif M. Sultanov [b], Ayaz A. Efendiev [b], Wolfgang Schuhmann [a,*]

[a] *Anal. Chem. — Elektroanalytik and Sensorik; Ruhr-Universität Bochum, D-44780 Bochum, Germany*
[b] *Institute of Chemical Problems of Azerbaijan National Academy of Sciences, Az 1143, Baku, Azerbaijan*

Received 3 March 2006; received in revised form 31 August 2006; accepted 14 September 2006
Available online 26 September 2006

Abstract

The integration of flexible anchoring groups bearing imidazolyl or pyridyl substituents into the structure of electrodeposition paints (EDP) is the basis for the parallel synthesis of a library containing 107 members of different cathodic and anodic EDPs with a high variation in polymer properties. The obtained EDPs were used as immobilization matrix for biosensor fabrication using glucose oxidase as a model enzyme. Amperometric glucose sensors based on the different EDPs showed a wide variation in their sensor characteristics with respect to the apparent Michaelis–Menten constant (K_M^{app}) representing the linear measuring range and the maximum current (I_{max}^{app}). Based on these results first assumptions concerning the impact of different side chains in the EDP on the expected biosensor properties could be obtained allowing for an improved rational optimization of EDPs used as immobilization matrix in amperometric biosensors.

Keywords: Electrodeposition paints; Polymer library; Functionalization; Parallel synthesis; Immobilization; Biosensor optimization

1. Introduction

The modification of immobilization material for preparation of amperometric biosensors constitutes an important step in the development of an optimal biosensor architecture for a specific application. The immobilization matrix predominantly defines the properties of amperometric biosensors since they secure the tight fixation of the biological recognition element at the electrode surface concomitantly guaranteeing the accessibility of the immobilized enzyme for its substrate and fast electron transfer between the immobilized enzyme and the electrode surface either via defined electron-transfer pathways using integrated redox relays or by means of free-diffusing redox mediators. An optimal immobilization material for amperometric biosensors should also possess additional features such as appropriate thermal and mechanical stability, protein-friendly environment, eventually suitable binding sites for the coordinative or covalent binding of redox mediators, biocompatibility, high permeability for fast substrate and product diffusion, internal cross-linking capacities as well as the ability to be locally deposited on predefined support surfaces in a controllable and reproducible fabrication process. In order to achieve these requirements, a variety of materials and techniques have been intensively investigated ranging from manual (drop- or dip-coating [1–3]) to non-manual immobilization processes (screen-printing [4], spin-coating followed by photolithographic structuring and lift-off [5], piezo-actuated micro-dispensing [6]). The main focus was on the investigation of the co-deposition of enzymes with polymeric materials on different electrode materials. For example, glucose oxidase was immobilized within a hydrophilic latex film containing hydroxyl or gluconamide groups [7] or the integration of long alkoxide spacers

* Corresponding author. Tel.: +49 234 3226200; fax: +49 234 3214683.
E-mail address: wolfgang.schuhmann@rub.de (W. Schuhmann).

1567-5394/$ - see front matter © 2006 Elsevier B.V. All rights reserved.
doi:10.1016/j.bioelechem.2006.09.004

into clay, silicate or glass was used for developing of flexible and controllable porous inorganic–organic matrices for biosensor applications [3,8,9]. It was shown that the integration of carboxylic acid units into hydrophobic poly-pyrrole films led to a significant increase in the related glucose sensor sensitivity [10] and that quarternization of pyridine units in redox hydrogels based on Os-complex modified poly(vinylpyridine) with hydrophilic groups such as 2-bromethanol or 3-brompropionic acid strongly improved the sensor characteristics [11,12].

Although many efforts were undertaken to gain in-depth knowledge of the complex parameter space influencing biosensor properties, still a rational design of immobilization matrices together with possibilities of chemical functionalization and addressability of the immobilization site is not possible. Thus, biosensor optimization is mainly done based on non-quantified expert knowledge in a trial and error variation of main influencing parameters.

Recently, we have introduced the application of anodic and cathodic electrodeposition paints (EDP) as immobilization matrices for amperometric biosensors [13–19]. EDPs can be precipitated exclusively on the electrode surface by changing the polymer charge imposing an electrochemically induced pH-value modulation in the diffusion zone in front of the electrode surface. During the formation of the polymer layer, enzymes present in the deposition solution are simultaneously entrapped within the ramified polymer network. The formed EDP layers show hydrogel properties due to their swelling in aqueous solution thus allowing for fast diffusional mass transport of the substrate to the site of the immobilized enzyme. Often polymer hydrogels are additionally stabilizing the three-dimensional structure of proteins enabling an improved sensor stability. Functionalization of EDPs has been thoroughly investigated for corrosion applications. Integration of carboxylic groups, tertiary amine groups or hydroxyl groups at the EDP backbone led to better adhesion and cohesion of EDP films on metal surfaces [20,21]. Hence, it is anticipated that the functionalization of EDPs will result in improved properties of the polymer layers also for biosensor applications.

In this communication, a synthesis strategy for the parallel formation of functionalized EDPs is presented. A number of functionalized monomers containing imidazolyl or pyridyl residues in the side chains were synthesized and subsequently copolymerized with a variety of comonomers following a combinatorial approach under formation of an EDP library containing 107 anodic and cathodic EDPs. The obtained polymers were evaluated with respect to their applicability in amperometric glucose oxidase-based biosensors and attempts to deduce a basic understanding of the influence of the polymer composition on the biosensor characteristics were performed.

2. Experimental section

2.1. Chemicals and materials

Di-tert.-butyl-hydroperoxide (DTBP), styrene (St), anhydrous acrylic acid (AA), *n*-butylacrylate (BA), methyl methacrylate (MMA), cyclohexyl methacrylate (CHMA), 2-ethylhexylmethacrylate (EHA), 4-pycolinamine (PA) were purchased from Fluka Chemie (Buchs, CH). Methyl acrylate (MA) and ethyl acrylate (EA) were obtained from Acros (Geel, B). 2-(dimethylamino)ethylmethacrylate (DMAEMA, 98%) was purchased from Sigma (Deisenhofen, D). 1,2-epoxy-5-hexene (EPH, 97%), *N*-vinylimidazole (VI), allyl glycidyl ether (AGE), 1-(3-aminopropyl)-imidazole (API, 98%) were obtained from Sigma Aldrich Chemie (Steinheim, D). 1,2-epoxy-9-decene (EPD, 96%) was obtained from Lancaster Synthesis (Eastgate, UK). D-(+)-glucose, isopropanol, KCl, NaOH, KOH, NaCl, HPLC grade water, imidazole, Na_2HPO_4, KH_2PO_4, K_2HPO_4, HCl (36–38%) were purchased from J.T. Baker (Deventer, NL). Glucose oxidase (GOx, EC 1.1.3.4, type XS, 100 000–250 000 units/g of solid, from *Aspergillus niger*) was obtained from Sigma (Deisenhofen, D). All chemicals were used as received.

2.2. Electrodes and electrochemical equipment

Constant potential amperometry was carried out in a conventional three-electrode electrochemical cell connected to a PED 300 bipotentiostat (Biometra, Göttingen, D) or a model 1030 electrochemical analyzer (CH Instruments, Austin, Tx, USA) using a Ag/AgCl/3 M KCl reference electrode and a Pt wire counter electrode. 1 mm diameter Pt disk electrodes sealed in glass were used as working electrodes. All potentials are referred to the Ag/AgCl/3 M KCl reference electrode.

2.3. Gas chromatography–mass spectrometry

A HP5890 (Hewlett-Packard, Böblingen, D) gas chromatograph connected to a mass spectrometer (HP5970 series mass selective detector) was used to characterize the synthesized functionalized monomers. The gaschromatographic separation was done using a DBxLB-mittelpolar 8–12% diphenylpolysiloxane capillary column (30 m in length × 0.25 mm internal diameter with 0.25 μm film thickness) using a temperature program starting at 60 °C for 2 min, then increasing the temperature to 300 °C at a rate of 15 °C min^{-1}, and holding at 300 °C for 3 min. Helium was used as carrier gas at a flow rate of 1 ml min^{-1} and a split ratio of 1/90. The injector and detector temperature was 250 °C.

2.4. Synthesis of imidazole-modified monomers

2.4.1. Synthesis of 1-imidazole-1-yl-hex-5-en-2-ol (EPH-Im) and 1-imidazole-1-yl-hex-5-en-3-oxy-2-ol (AGE-Im)

247 mmol of allyl glycidyl ether (AGE) or 99 mmol 1,2-epoxy-5-hexene (EPH) was added dropwise to 240 mmol of

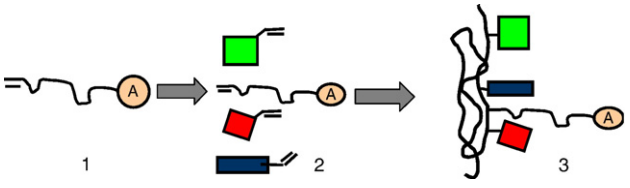

Fig. 1. Schematic representation of the synthetic strategy for integrating functional side chains within EDPs. 1. Synthesis of functionalized monomers; 2. mixing with a set of monomers with side chains of different properties; 3. copolymerization leads to a functionalized EDP.

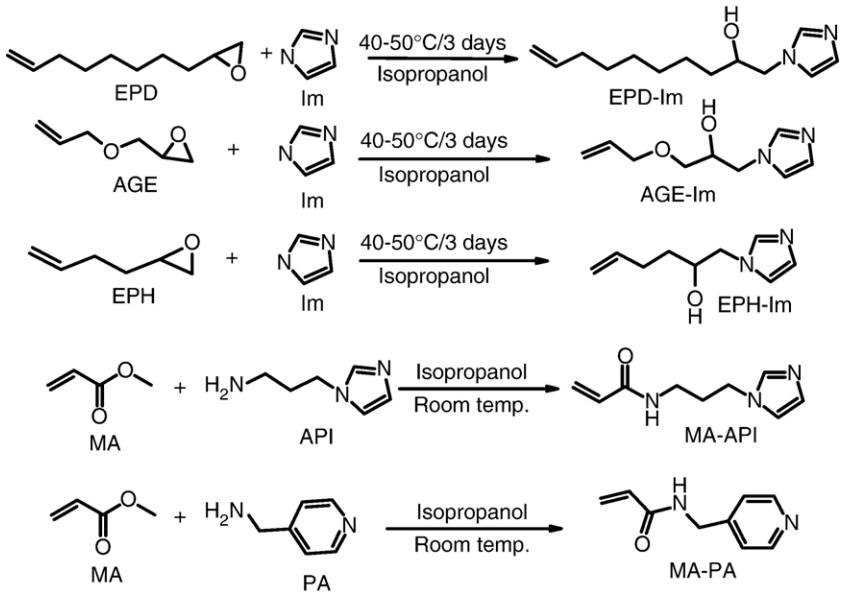

Fig. 2. Synthesis of imidazolyl and pyridyl modified monomers as building block for EDPs. *EPH-Im*: 1-imidazole-1-yl-hex-5-en-2-ol; *AGE-Im*: 1-imidazole-1-yl-hex-5-en-3-oxy-2-ol; *EPD-Im*: 1-imidazole-1-yl-dec-9-en-2-ol; *MA-API*: *N*-(3-imidazole-1-yl-propyl)-acrylamid; *MA-PA*: *N*-pyridin-4-yl-methyl-acrylamid.

imidazole (90 mmol imidazole) and dissolved in 30 ml (27 ml) isopropanol during 1 h. The mixture was stirred for 3 days at 40–50 °C to complete the reaction. After evaporation of the solvent a yellow and oily product was obtained. The analysis of the product by GC–MS showed two peaks corresponding to AGE (EPH) and AGE-Im (EPH-Im), respectively. No peak of residual imidazole was observed. The crude product was used without further purification.

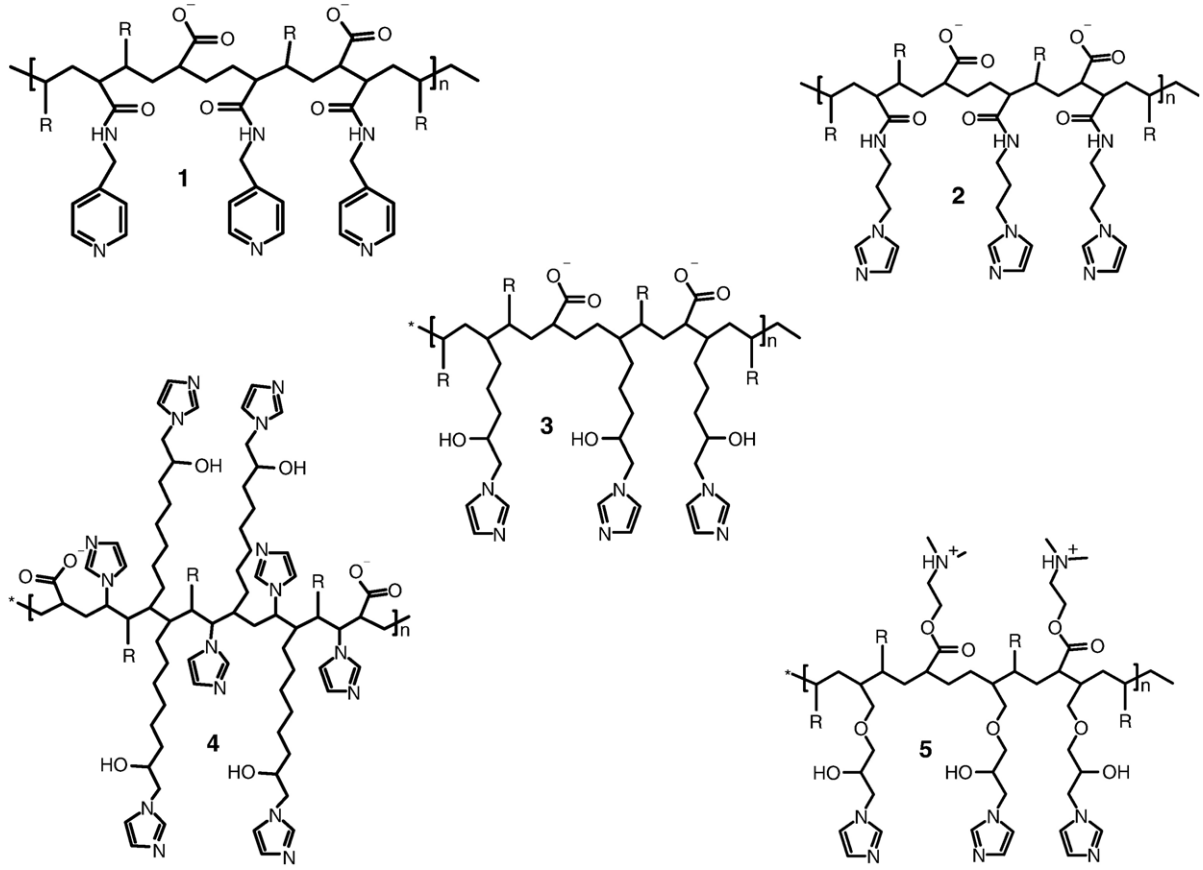

Fig. 3. Typical EDP structures containing the synthesized imidazolyl and pyridyl containing monomers (R: MMA; BA; CHMA; EHA; EA; St).

Table 1
Monomer composition of the polymer members of the EDP library together with the properties of the derived amperometric glucose biosensors

Polymer	Monomer (mmol)					K_M^{app}/mM	I_M^{app} /nA
CP1	AGE-Im (2)	BA (4)	DMAEA (4)	MMA (2)		–	–
CP2	AGE-Im (1)	BA (5)	DMAEA (4)	MMA (2)		–	–
CP3	AGE-Im (3)		DMAEA (4)	St (3)	EHA (2)	–	–
CP4	AGE-Im (3)	St (3)	DMAEA (4)	MMA (1)	EHA (2)	–	–
CP5	AGE-Im (3)	BA (4)	DMAEA (4)	MMA (1)		24.6±2.1	93.4±3.8
CP6	AGE-Im (4)		DMAEA (4)	MMA(4)		17.4±3.1	173.7±11.2
CP7	AGE-Im (3)	BA (5)	DMAEA (4)			16.7±1.5	106.8±4.2
CP8	AGE-Im (5)	BA (2)	DMAEA (4)	MMA (1)		13.4±2.0	61.2±3.2
CP9	AGE-Im (4)	BA (2)	DMAEA (4)	MMA (2)		24.9±2.1	250.3±3.6
CP10	AGE-Im (4)	BA (4)	DMAEA (4)			20.4±2.2	140.4±5.8
CP11	AGE-Im (5)	BA (2)	DMAEA (5)			18.2±2.2	87.1±3.8
CP12	AGE-Im (5)	BA (3)	DMAEA (4)			18.2±1.1	430.3±10.1
CP13	AGE-Im (6)		DMAEA (4)	MMA (2)		18.1±1.2	483.9±11.9
CP14	AGE-Im (3)	BA (4)	DMAEA (4)	St (1)		15.4±1.6	310.9±11.6
CP15	AGE-Im (4)	BA (3)	DMAEA (4)	MMA (1)		11.9±0.9	273.9±6.7
CP16	AGE-Im (4)	BA (2)	DMAEA (4)	St (2)		15.2±3.7	219.9±19.0
CP17	AGE-Im (4)		DMAEA (4)	EA (4)		2.0±0.3	1518.8±47.0
CP18	AGE-Im (6)	BA (2)	DMAEA (4)			5.5±0.5	278.8±7.1
CP19	AGE-Im (4)	BA (3)	DMAEA (4)	St (1)		2.0±0.7	8.6±0.6
CP20	AGE-Im (6)		DMAEA (4)	EHA (2)		25.1±2.8	208.3±10.6
CP21	AGE-Im (5)	St (2)	DMAEA (4)	MMA (1)		8.3±0.7	524.4±15.5
CP22	AGE-Im (5)	St (3)	DMAEA (4)			14.5±1.5	843.7±30.1
CP23	AGE-Im (6)	St (1)	DMAEA (4)	MMA (1)		13.1±2.2	840.3±49.2
CP24	AGE-Im (4)	BA (2)	DMAEA (4)	EA (2)		5.1±1.1	630.3±1.1
CP25	AGE-Im (4)	BA (3)	DMAEA (4)	EA (1)		5.3±1.3	281.8±18.1
CP26	AGE-Im (5)		DMAEA (4)	MMA (1)	CHMA (2)	12.9±1.9	412.1±20.5
CP27	AGE-Im (5)		DMAEA (4)		EHA (3)	9.4±1.1	36.6±1.3
CP28	AGE-Im (6)		DMAEA (4)	MMA (1)	CHMA (1)	6.0±1.2	308.7±17.2
CP29	AGE-Im (5)	BA (2)	DMAEA (4)		CHMA (1)	1.8±0.2	266.1±4.4
CP30	AGE-Im (5)	BA (2)	DMAEA (4)		EHA (1)	4.0±0.7	869.4±36.5
CP31	AGE-Im (5)		DMAEA (4)	MMA (2)	CHMA (1)	–	–
CP32	AGE-Im (3)	BA (4)	DMAEA (4)		CHMA (1)	1.4±0.1	180.5±1.6
CP33	AGE-Im (4)		DMAEA (4)	EA (2)	CHMA (2)	5.7±0.6	136.1±3.9
CP34	AGE-Im (5)		DMAEA (4)	EA (1)	CHMA (2)	13.6±0.7	336.3±5.9
CP35	AGE-Im (6)		DMAEA (4)	EA (1)	CHMA (1)	7.6±0.6	195.0±4.9
CP36	AGE-Im (6)		DMAEA (4)	EA (1)	EHA (1)	15.3±1.1	275.8±7.2
CP37	AGE-Im (5)		DMAEA (4)	EHA (2)	CHMA (1)	9.9±1.7	290.6±16.9
CP38	AGE-Im (5)		DMAEA (4)	EHA (1)	CHMA (2)	5.7±0.4	337.6±6.7
CP39	AGE-Im (4)	BA (2)	DMAEA (4)		CHMA (2)	11.4±0.7	490.6±10.5
CP40	AGE-Im (5)	BA (1)	DMAEA (4)		CHMA (2)	5.3±0.7	689.1±23.3
CP41	AGE-Im (6)		DMAEA (4)		CHMA (2)	0.3±0.1	552.7±5.3
CP42	AGE-Im (5)		DMAEA (4)		CHMA (3)	0.8±0.1	459.2±5.3
CP43	AGE-Im (4)		DMAEA (4)		CHMA (4)	2.0±0.2	325.3±6.1
CP44	AGE-Im (4)		DMAEA (4)	St (4)		0.6±0.2	606.3±16.3
CP45	AGE-Im (7)		DMAEA (4)		CHMA (1)	10.9±1.1	126.3±4.4
CP46	AGE-Im (6)		DMAEA (4)	St (1)	EHA (1)	9.5±0.8	271.1±7.7
CP47	AGE-Im (6)		DMAEA (4)	MMA (1)	EHA (1)	19.0±3.2	266.2±16.4
CP48	AGE-Im (6)		DMAEA (4)	CHMA (1)	EHA (1)	0.3±0.2	114.9±4.5
CP49	AGE-Im (6)	BA (1)	DMAEA (4)		EHA (1)	21.7±2.4	401.1±17.3
CP50	AGE-Im (4)	MMA(1)	DMAEA (4)	St (1);BA(1)	EA (1)	0.6±0.1	423.7±2.4
AP51	AGE-Im (3)	BA (6)	AA (3)			12.1±0.8	521.2±11.8
AP52	AGE-Im (3)	BA (5)	AA (3)	St (1)		8.8±0.8	207.2±6.1
AP53	AGE-Im (3)	BA (5)	AA (3)	CHMA (1)		13.7±1.0	395.2±9.9
AP54	AGE-Im (3)	BA (5)	AA (3)	MMA (1)		10.4±1.4	444.2±19.2
AP55	AGE-Im (3)	BA (4)	AA (3)	St (2)		9.9±0.9	538.9±16.0
AP56	EPH-Im (3)	BA (6)	AA (3)			5.8±0.4	745.2±14.2
AP57	EPH-Im (3)	BA (5)	AA (3)	St (1)		10.4±0.6	487.1±8.7
AP58	EPH-Im (3)	BA (5)	AA (3)	CHMA (1)		3.1±0.1	1035.2±6.8
AP59	EPH-Im (3)	BA (5)	AA (3)	MMA (1)		6.4±0.2	1255.7±13.6
AP60	EPH-Im (3)	BA (4)	AA (3)	St (2)		–	–
AP61	EPD-Im (4)	VI (5)	AA (3)			4.6±0.6	76.8±2.5
AP62	EPD-Im (3)	VI (5)	AA (3)	MMA (1)		5.5±0.5	108.7±2.7
AP63	EPD-Im (3)	VI (4)	AA (3)	MMA (2)		8.9±1.2	72.3±3.0
AP64	EPD-Im (3)	VI (3)	AA (3)	MMA (3)		6.2±1.2	47.1±2.6

Table 1 (*continued*)

Polymer	Monomer (mmol)					K_M^{app}/mM	I_M^{app} /nA
AP65	EPD-Im (3)	VI (2)	AA (3)	MMA (4)		3.8±0.6	25.2±0.9
AP66	MA-API (3)	BA (6)	AA (3)			–	–
AP67	MA-API (3)	BA (5)	AA (3)	CHMA (1)		7.6±0.6	719.3±16.8
AP68	MA-API (3)	BA (5)	AA (3)	MMA (1)		2.5±0.2	1303.5±30.3
AP69	MA-API (3)	BA (4)	AA (3)	St (2)		–	–
AP70	MA-API (3)	BA (3)	AA (3)	MMA (3)		15.2±2.2	365.3±16.3
AP71	MA-API (3)	BA (4)	AA (3)	MMA (2)		5.8±0.5	374.5±9.6
AP72	MA-API (3)	BA (3)	AA (3)	CHMA (2)	MMA (1)	–	–
AP73	MA-API (3)	BA (4)	AA (3)	CHMA (2)		–	–
AP74	MA-API (3)	BA (3)	AA (3)	CHMA (3)		–	–
AP75	MA-API (3)	BA (3)	AA (3)	St (2)		–	–
AP76	MA-API (3)	BA (3)	AA (3)	St (2)	MMA (1)	–	–
AP77	MA-API (3)	BA(4)	AA (3)	CHMA (1)		4.7±0.8	446.0±19.0
AP78	MA-PA (3)	BA (3)	AA (3)	MMA (3)		12.6±0.9	269.0±6.7
AP79	MA-PA (3)	BA (3)	AA (3)	St (1)	CHMA (2)	–	–
AP80	MA-PA (3)	BA (4)	AA (3)	CHMA (2)		–	–
AP81	MA-PA (3)	BA (3)	AA (3)	CHMA (3)	MMA (1)	–	–
AP82	MA-PA (3)	BA (4)	AA (3)	St (2)		7.6±0.1	168.0±3.1
AP83	MA-PA (3)	BA (3)	AA (3)	St (2)	CHMA (1)	11.7±0.7	241.0±4.5
AP84	MA-PA (3)	BA (4)	AA (3)	St (1)		–	–
AP85	MA-PA (3)	BA (5)	AA (3)	MMA (1)		–	–
AP86	MA-PA (3)	BA (2)	AA (3)	MMA (3)	EHA (1)	–	–
AP87	MA-PA (3)	BA (3)	AA (3)	MMA (2)	EHA (1)	–	–
AP88	MA-PA (3)	BA (3)	AA (3)	CHMA (2)	MMA (1)	7.6±2.3	170.3±4.6
AP89	MA-PA (3)	BA (4)	AA (3)	CHMA (1)	EHA (1)	1.8±0.3	70.7±6.4
AP90	MA-PA (3)	BA (3)	AA (3)	CHMA (3)		–	–
AP91	MA-PA (3)	BA (3)	AA (3)	St (2)	EHA (1)	–	–
AP92	MA-PA (3)	BA (3)	AA (3)	St (1); EHA(1)	CHMA (1)	–	–
AP93	MA-PA (3)	BA (3)	AA (3)	St (2)	MMA (1)	–	–
AP94	MA-PA (3)	BA (3)	AA (3)	CHMA (1)	EHA (1)	1.1±0.2	105.5±36.0
AP95	MA-PA (3)	BA (4)	AA (3)	CHMA (1)		2.1±0.2	266.3±5.6
AP96	MA-PA (3)	BA (6)	AA (3)	CHMA (1)		–	–
AP97	MA-PA (3)	BA (6)	AA (3)		MMA (1)	0.2±0.0	960.3±26.4
AP98	MA-API (3)	BA (4)	AA (3)	CHMA (1)	MMA (1)	2.2±0.1	1118.9±43.0
AP99	MA-API (3)	BA (5)	AA (3)		MMA (2)	0.7±0.1	1424.3±20.5
AP100	MA-API (3)	BA (3)	AA (3)	CHMA (1)	St (1); MMA(1)	–	–
AP101	MA-API (3)	BA (5)	AA (3)	St (1)		2.2±0.1	882.7±10.3
AP102	MA-PA (3)	BA (5)	AA (3)	MMA (1)		–	–
AP103	MA-PA (3)	BA (4)	AA (5)			6.9±0.5	198.3±4.4
AP104	MA-PA (4)	BA (4)	AA (4)			9.3±0.2	261.9±2.6
AP105	MA-PA (4)	BA (5)	AA (3)			11.7±1.1	249.8±7.8
AP106	EPH-Im (3)	BA (5)	AA (3)	EA (1)		35.5±3.5	196.2±8.4
AP107	EPH-Im (3)	BA (5)	AA (3)	VI (1)		30.5±4.2	416.5±3.6

MS data: AGE-Im: RT 12.2 min; major fragments(%)–mass: 100%–41; 98.6%–82; 28.4%–54; 18.9%–69; 14.9%–126; 20.3%–109; 9.45%–141; 4%–152; 3.4%–181; 18.2%–29; 3.4%–165.

EPH-Im: RT 11.8 min; major fragments(%)–mass: 100%–81; 58.8%–41; 39.2%–29; 35.3%–55; 37.2%–69; 5.9%–95; 7.8%–112; 8.3%–151; 5.9%–166.

2.4.2. Synthesis of 1-imidazole-1-yl-dec-9-en-2-ol (EPD-Im)

60 mmol of 1,2-epoxy-9-decene (EPD) was added dropwise to 65 mmol of imidazole dissolved in 17 ml isopropanol during 1 h. The mixture was stirred for 3–7 days at 40 °C to accelerate the reaction. The product obtained after removal of the solvent was used without further purification.

MS data: EPD-Im: RT 15 min; major fragments(%)–mass: 100%–82; 62.2%–41; 48.6%–55; 40.5%–69; 1%–95; 28.4%–109; 16.2%–122; 10.8%–151; 6.7%–165; 9.4%–179; 8.1%–193; 6.7%–205; 12.2%–221; 29.7%–29.

2.4.3. Synthesis of N-(3-imidazole-1-yl-propyl)-acrylamid (MA-API) and N-pyridin-4-yl-methyl-acrylamid (MA-PA)

100 mmol 1-(3-aminopropyl)-imidazole (API) or 4-pycolinamine (PA), respectively, were mixed with 40 ml isopropanol in a 100 ml round-bottom flask. 105 mmol methyl acrylate (MA) was dissolved in 20 ml isopropanol and added dropwise to the mixture under stirring at room temperature during 24 h. Excess of unreacted MA was removed from the yellowish and oily product by rota-evaporation.

MS data: *MA-API*: RT 14.0 min; major fragments(%)–mass: 100%–42; 27%–55; 55%–70; 49%–82; 25%–95; 20%–110; 20%–124; 2%–138; 24%–152; 3%–180. *MA-PA*: RT 12.0 min; major fragments(%)–mass 100%–92; 41%–42; 17%–51;

10%–60; 37%–65; 10%–70; 7%–79; 14%–84; 78%–107; 76%–121; 2%–133; 1%–161.

2.4.4. Synthesis of EDP containing monomers with imidazolyl or pyridyl side chains

EDP was prepared following a parallel synthesis scheme as reported previously [14]. Radical copolymerization of a mixture of polymer building blocks such as EHA, BA, St, MMA, EA, MA, VI, CHMA, AGE-Im, EPH-Im, EPD-Im, MA-IPA, MA-PA was initiated by the radical starter DTBP in the presence of a small amount of solvent (250 µl water; 250 µl isopropanol). Basically, the mixture consisting of different monomers; solvent and initiator was stirred and heated for 5 h at 80 °C in a specially designed reaction tube with reflux condenser. Up to 16 polymers with different monomer composition could be prepared in parallel. By varying the composition and relative amounts of the monomers a library containing 107 members of different EDPs was synthesized. The viscosity of the obtained polymers was reduced by adding water (typically 3 ml) and vigorous stirring overnight for homogenization. Two basically different types of EDPs were prepared: anodic polymers based on AA as main pH-dependent residue and cathodic polymers based on DMAEMA.

2.5. Biosensors fabrication and evaluation

The copolymer suspensions were pre-diluted with water (1:1 or 4:1), and 500 µl of the functionalized EDP suspension were thoroughly mixed with 100 µl of GOx solution (5 mg ml^{-1}). Electrochemical polymer deposition was initiated on a 1 mm diameter Pt disk electrode by means of a potential pulse sequence causing water oxidation (for anodic EDP) or water reduction (for cathodic EDP) at the electrode surface under concomitant liberation of H^+ or OH^- ions. 30 potential pulse cycles to −2 V for 0.2 s followed by a relaxation phase at 0 V for 5 s were applied in case of cathodic EDPs whereas potential pulse profiles to +2.2 V for 0.2 s, 0.8 V for 1 s followed by a relaxation phase at 0 V for 5 s were used for the precipitation of anodic paints. All enzyme electrodes were evaluated in an electrochemical cell with 20 ml 0.1 M PBS, pH 7.2 equipped with a Pt counter and a Ag/AgCl/3 M KCl reference electrode. For constant-potential amperometry the biosensors were poised to a potential of +600 mV vs. Ag/AgCl 3 M KCl reference electrode in order to oxidize enzymatically generated H_2O_2.

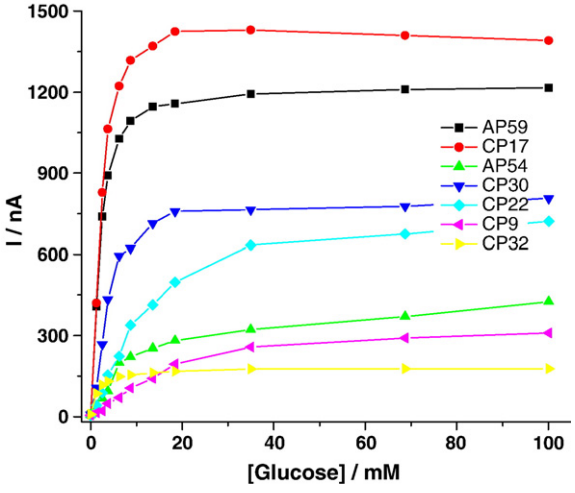

Fig. 4. Glucose calibration graphs from biosensors obtained using different functionalized electrodeposition paints as immobilization matrix for glucose oxidase (600 mV; oxidation of enzymatically generated H_2O_2).

3. Results and discussion

The solubility of anodic and cathodic polymers is mainly controlled by the pH value and the monomer composition contributing with steric requirements and hydrophilic or hydrophobic properties of the side chains. Thus, an EDP which is suitable as immobilization matrix for amperometric biosensors will only be successfully synthesized if a compromise between the influencing parameters of all integrated monomers is found. Moreover, in order to allow for a later modification of the polymer by e.g. coordinative binding of suitable redox complexes or covalent cross-linking using bifunctional molecules functional groups should be integrated already during the polymer formation reaction. The most straightforward approach to integrate specific functions at the polymer backbone is to synthesize monomers with the desired functional side chains which are then copolymerized with a set of other monomers (Fig. 1). Due to the complex interaction of the properties of all monomers the polymer characteristics cannot be easily predicted and thus, assuming that electrochemically induced pH modulation successfully leads to a polymer precipitation at the electrode surface, also the characteristics of the related biosensors cannot be predicted. In order to improve the knowledge about the impact of the various monomers and especially the synthesized functional monomers the preparation of a library of anodic and cathodic EDPs with a high variability in the monomer composition was anticipated.

3.1. Functionalization of electrodeposition paints

3.1.1. Synthesis of monomers with functional side chains

The used monomers bearing flexible spacer chains often contribute to the overall polymer properties by improving the plasticity and homogeneity [22,23]. Therefore the integration of monomers exhibiting good solubility both in aqueous and organic solvents or allowing for a combination with a big variety of other suitable monomers under formation of EDPs provides the possibility for controlling of physical and chemical properties of the resulting polymer film such as glass transition temperature, permeability, viscosity, hydrogel properties. Thus, different strategies were investigated aiming on the synthesis of monomers containing functional side chains.

First, condensation of carbodiimide and *N*-hydroxysuccinimid activated [24–26] carboxylic acid residues (e.g. of acrylic acid; AA) with 1-(3-aminopropyl)-imidazole (API) or 4-pycolinamine (PA) in organic solvents was exploited. However,

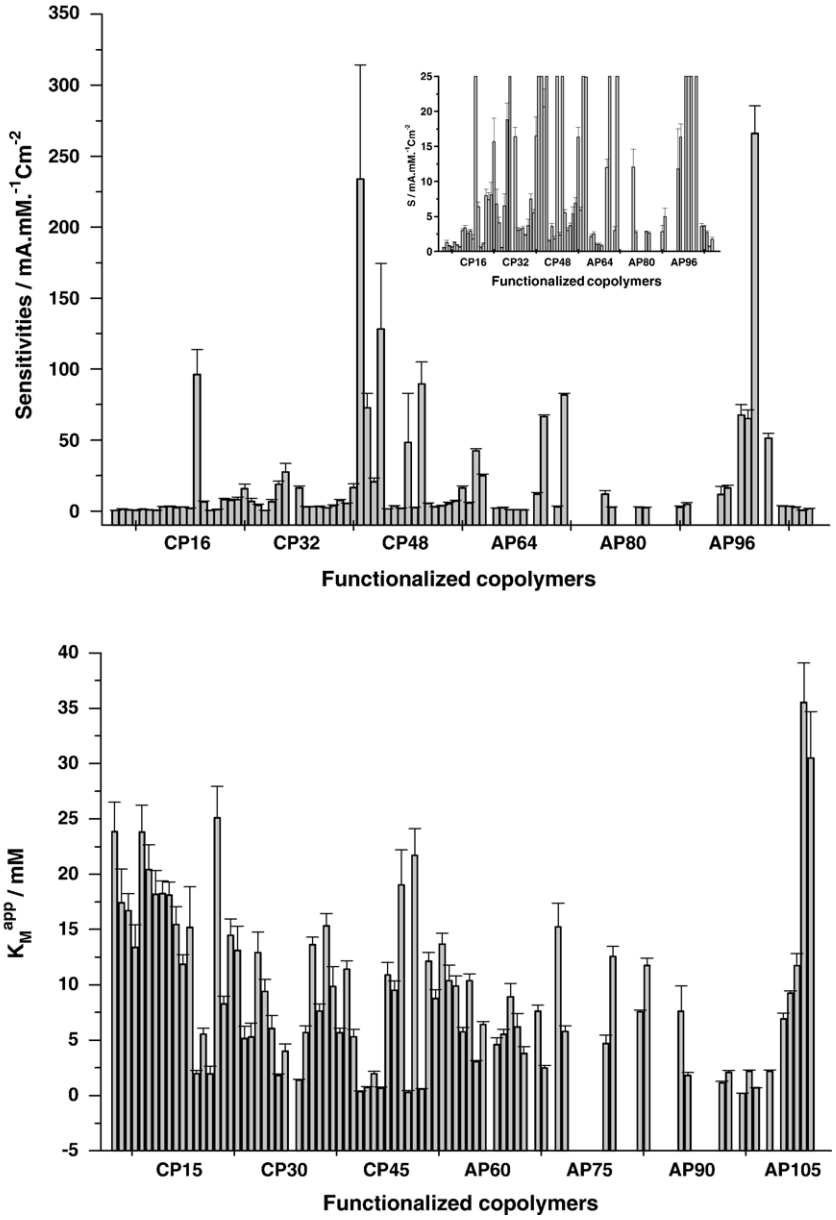

Fig. 5. Sensitivity (S/mA mM^{-1} cm^{-2}) and linear range (K_M^{app}/mM) of each glucose biosensor fabricated by using different members of the EDP library as immobilization matrix for the entrapment of glucose oxidase.

this attempt exhibited disadvantages such as the at least partly occurring homopolymerization of the monomers already during the modification step, the presence of residual impurities in the product preventing the copolymerization reaction, and the alteration of the pH-dependent solubility due to a decreased number of charged side chains. Thus, alternative approaches were envisaged aiming on the synthesis of functionalized monomers in a simple and efficient single step using the same solvent for the modification, later for the copolymerization reaction and finally for the immobilization of the biological recognition element within the precipitated polymer layer.

Vinyl epoxy monomers were reacted with imidazole under formation of imidazolyl functionalized monomers. Alternatively, acrylic acid methyl ester (MA) was reacted with 1-(3-aminopropyl)-imidazole (API) or 4-pycolinamine (PA). After the modification reaction, excess MA was removed using evaporation under reduced pressure. The reaction equations for the synthesis of a variety of spacer-modified monomers with different lengths of the side chains are shown in Fig. 2. Epoxy groups react efficiently and selectively (more than 95% yield) with imidazole at ambient temperature. The synthesis can be accelerated by heating the reaction mixture to 40–50 °C.

3.1.2. Synthesis of a library of functionalized anodic and cathodic EDPs

A simplified synthesis strategy was employed for the copolymerization reaction of imidazolyl and pyridyl functionalized monomers with a selection of hydrophobic and hydrophilic comonomers. Basically the synthesis procedure of the corresponding anodic or cathodic electrodeposition paint

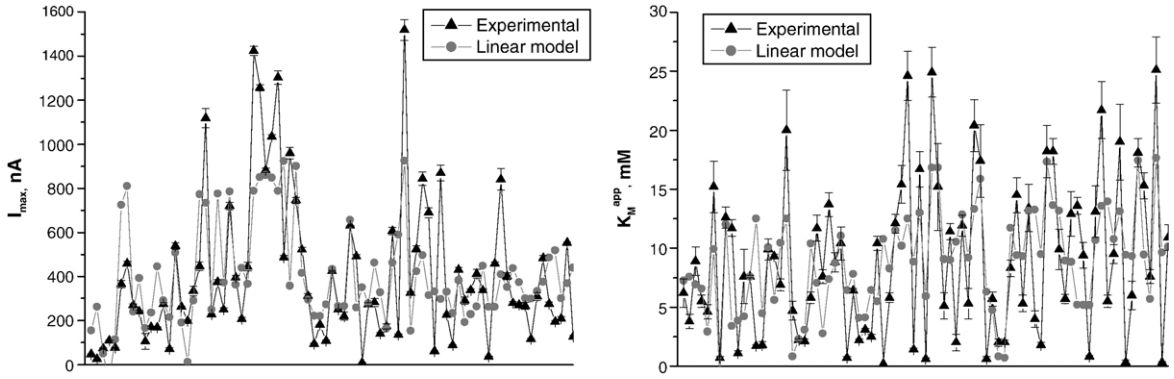

Fig. 6. Comparison of the experimental and predicted values of I_{max}^{app} and K_M^{app} for the glucose biosensors fabricated with the different polymers from the EDP library.

involved heating of a premixed solution of monomers, solvent, initiator, acid or base for neutralization to 80 °C for 5 h. The obtained anodic or cathodic copolymers were diluted by means of HPLC grade water and continuously stirred for 24 h to form a stable aqueous EDP emulsion. The use of a solvent mixture consisting of isopropanol and water helped to overcome the incompatibility between the solubility of the monomers. Although numerous mathematical formulations have been established in the past years which correlate the chemical composition of a polymer to its properties [27–29], it is little known about the properties of the synthesized copolymers. Thus, by varying the monomer composition in the synthesized copolymers in a combinatorial way a library consisting of 107 anodic and cathodic EDPs was synthesized (Fig. 3) following a previously described parallel synthesis regime [14].

The composition of each member of the polymer library is listed in Table 1. Due to the branched structure of the obtained EDPs and the presence of hydrophilic groups most of the polymers exhibit hydrogel properties thus facilitating diffusional mass transport e.g. of the substrate to the site of the entrapped enzyme. Most of the polymers (CP1–CP50; AP61–AP65) were diluted with 3 ml water to form a stable emulsion. However, a large quantity of water (~16 ml) was necessary to obtain a stable emulsion in the case of anodic resins containing AGE-Im while comparable polymers based on EPH-Im required only 5 ml water. The cathodic polymers CP1–CP4 were solid at room temperature and hence not applicable for biosensor fabrication.

3.2. Entrapment of glucose oxidase within functionalized electrodeposition paints

For the fabrication of EDP-based biosensors glucose oxidase (100 µl; 5 mg ml^{-1}) is mixed with 500 µl of copolymer suspension. Using a miniaturized electrochemical cell with a 1 mm Pt disk electrode as working electrode, a Pt wire counter electrode and a Ag/AgCl reference electrode the pH value was locally changed in the diffusion layer in front of the working electrode by applying a potential pulse sequence to either −2 V for generation of OH^- ions or +2.2 V for the formation of H^+. The local pH modulation leads to a change in the polymer solubility and consequently to a precipitation of the polymer entrapping concomitantly the enzyme. As a matter of fact, the different properties of the synthesized polymers lead to wide variations in the polymer film thickness and consequently the amount of active enzyme present in the polymer film. However, in order to obtain first hints on the properties of the different polymer films for biosensor applications, for all cathodic paints and all anodic paints the same number of deposition pulses was used, assuming that the properties of the obtained glucose biosensors reflect at least to a certain extent the properties of the polymer film. As expected, the glucose biosensors showed significant differences with respect to the maximum current at substrate saturation (I_{max}^{app}) and the local concentration of the substrate at the site of the enzyme which is mainly reflected by the apparent Michaelis constant (K_M^{app}) in dependence from the composition of the used polymer (Fig. 4). I_{max}^{app} and K_M^{app} values for all glucose biosensors are summarized in Table 1. Obviously, the composition of the used polymer as well as the relative amount of a distinct monomer within the polymer have a great impact on the biosensor properties and hence it should be feasible to select suitable polymers as immobilization matrix according to the anticipated sensor properties.

In general, biosensors based on cathodic paints showed wider linear detection ranges most probably due to the low hydrophilicity of DMAEA after deprotonation leading to a dense polymer layer concomitantly slowing down substrate diffusion. In contrast, the use of acrylic acid as monomer in anodic paints increased the hydrophilicity and polarity of the polymer. In combination with a facilitated swelling substrate diffusion is fast and hence a low K_M^{app} value is measured. CP20, AP106 and AP107 exhibited the widest linear range (K_M^{app} =25.1; 35.5; 30.5 mM, respectively). Exchanging EHA against CHMA (CP41) significantly reduces the linear range to K_M^{app} =0.3 mM and simultaneously improves the sensitivity of the corresponding glucose sensor by a factor of 213 times.

Replacing St (AP57) with CHMA (AP58), MMA (AP59), EA (AP106) or VI (AP107) led to higher sensitivities with still rather wide linear ranges for AP58 and AP59. Obviously, a decrease in hydrophobicity of the side chains allows for faster substrate diffusion and possibly leads to a more enzyme friendly

environment within the polymer layer. Replacing AGE-Im (AP51–AP55) with EPH-Im (AP56–AP60) led to a significant increase in sensitivity. Since AGE-Im is only distinguished from EPH-Im by one ether group in the side chain, this effect cannot be easily interpreted. However, obviously AGE-Im leads to a denser polymer with decreased substrate diffusion. Comparing AP60 [EPH-Im (3), AA (3), BA (4), St (2); $I_{max}^{app}=0$ nA] with AP55 [AGE-Im (3), AA (3), BA (4), St (2); $I_{max}^{app}=538.9$ nA] suggests that in contrast to AGE-Im the hydrophilicity of EPH-Im is not sufficient to compensate for the impact of St in the polymer. Thus, AP60 does not form a stable emulsion in aqueous solution and hence cannot be precipitated on an electrode surface under simultaneous entrapment of the enzyme. The use of a high amount of St (>10% of the monomers) often leads to polymers which cannot be solubilized in aqueous solution (CP3; AP60; AP70; AP77). This effect can be compensated for using AGE-Im and DMAEA in cathodic polymers (e.g. CP44) (Fig. 5).

Among the 107 copolymer members of the library, 80 members formed a stable suspension in water and could be precipitated upon local electrochemically induced pH-value changes. 27 copolymers of the library which often contain MA-API or MA-PA were either insoluble in aqueous solution or their solubility was too high for pH-induced precipitation in the presence of the enzyme. Indeed, it was difficult to adjust the balance between MA-API or MA-PA and hydrophobic comonomers for obtaining the required pH-dependent solubility. More than 70% of the biosensors based on the synthesized copolymers displayed sensitivities to glucose with less or equal to 10 mA mM^{-1} cm^{-2}, however, CP41 (234 mA mM^{-1} cm^{-2}) and AP99 (266 mA mM^{-1} cm^{-2}) showed a more than 20 times higher I_{max}^{app}. This difference in sensitivity and linear range demonstrates the high potential of EDP to optimize the immobilization material just by modulating its chemical composition.

To evaluate the dependence of the main properties of the obtained biosensors namely I_{max}^{app} and K_M^{app} from the monomer composition of the polymer multivariate regression analysis was carried out using a linear regression model. Based on the assumption that the biosensor characteristics are linearly dependent on the sum of the properties of the immobilization matrix such as hydrophilicity, hydrophobicity, viscosity, polymer film thickness etc. the specific property can be expressed as a combination of the impact of the monomer properties multiplied by a weight factor.

The weight factors of each monomer in a polymer were used as predictors for I_{max}^{app} and K_M^{app} as functions of the monomer composition at the fixed experimental conditions. The linear regression model has shown statistically significant correlation coefficients of 0.64 and 0.68 ($p=0.0003$ and $p=0.00002$, respectively), which indicate moderate correlation between experimental data and the linear model. For both dependent variables all predictors were found to be significant (with $p<0.05$). In Fig. 6 the experimental and predicted I_{max}^{app} and K_M^{app} for the different polymers are compared.

4. Conclusion

Although the correlation between the linear model and the experimental data is far from being sufficient the large number of polymers investigated in this study allows to draw conclusions on the impact of the properties of the monomers on the copolymer characteristics which are mainly determining the overall properties of the glucose biosensors. Presently, a significant increase in the reproducibility of the sensor formation is attempted by using an electrochemical robotic system [30] for high-throughput sensor fabrication and evaluation. In addition, the reproducibility of the polymer formation process will be optimized. By additionally changing the film thickness for each polymer the impact of the different polymer characteristics on the biosensor properties will be even better understood allowing for predicting with significantly improved correlation optimized polymer structures. This study clearly paves the road for more sophisticated automated polymer evaluation strategies.

Acknowledgements

This work is funded by the European Commission in the framework of INTAS 03–51–6278 and HPRN-CT-2002–00186.

References

[1] X. Yang, G. Johansson, L. Gorton, A glucose sensor made by chemically crosslinking glucose oxidase directly on the surface of a carbon electrode modified with Pd/Au for hydrogen peroxide electrocatalysis, Mikrochim. Acta 4 (1989) 9–16.
[2] U. Kunzelmann, H. Bottcher, Biosensor properties of glucose oxidase immobilized within SiO_2 gels, Sens. Actuators, B, Chem. 39 (1997) 222–228.
[3] B.Q. Wang, B. Li, Q. Deng, S.J. Dong, Amperometric glucose biosensor based on sol–gel organic–inorganic hybrid material, Anal. Chem. 70 (1998) 3170–3174.
[4] R. Nagata, K. Yokoyama, S.A. Clark, I. Karube, A glucose sensor fabricated by the screen-printing technique, Biosens. Bioelectron. 10 (1995) 261–267.
[5] S. Gernet, M. Koudelka, N.F. de Rooij, A planar glucose enzyme electrode, Sens. Actuators 17 (1989) 537–540.
[6] J.D. Newman, A.P.F. Turner, G. Marrazza, Ink-jet printing for the fabrication of amperometric glucose biosensors, Anal. Chim. Acta 262 (1992) 13–17.
[7] S. Cosnier, S. Szunerits, R.S. Marks, A. Novea, L. Puech, E. Perez, I. Rico-Lattes, A rapid and easy procedure of biosensor fabrication by micro-encapsulation of enzyme in hydrophilic synthetic latex films. Application to the amperometric determination of glucose, Electrochem. Commun. 2 (2000) 851–855.
[8] J.Z. Zhang, B. Li, Z.X. Wang, G.J. Cheng, S.J. Dong, Functionalized inorganic–organic composite material derivated by sol–gel for construction of mediated amperometric hydrogen peroxide biosensor, Anal. Chim. Acta 388 (1999) 71–78.
[9] S. Poyard, N. Jaffrezic-Renault, C. Martelet, S. Cosnier, P. Labbe, Optimization of an inorganic/bio-organic matrix for the development of new glucose biosensor membrane, Anal. Chim. Acta 364 (1998) 165–172.
[10] K. Habermüller, S. Reiter, H. Buck, T. Meier, J. Staepels, W. Schuhmann, Conducting redoxpolymer-based reagentless biosensors using modified PQQ-dependent glucose dehydrogenase, Mikrochim. Acta 143 (2003) 113–121.
[11] A. Heller, Crosslinked redox gels containing glucose oxidase for amperometric biosensor applications, Anal. Chem. 62 (1990) 258–263.
[12] B.A. Gregg, A. Heller, Redox polymer films containing enzymes. Glucose oxidase containing enzyme electrodes, J. Phys. Chem. 95 (1991) 5970–5975.
[13] C. Kurzawa, A. Hengstenberg, W. Schuhmann, Immobilization method for the preparation of biosensors based on pH shift-induced deposition of biomolecule-containing polymer films, Anal. Chem. 74 (2002) 355–361.
[14] B. Ngounou, S. Neugebauer, A. Frodl, S. Reiter, W. Schuhmann, Combinatorial synthesis of a library of acrylic acid-based polymers and

their evaluation as immobilisation matrix for amperometric biosensors, Electrochim. Acta 49 (2004) 3855–3863.
[15] S. Reiter, D. Ruhlig, B. Ngounou, S. Neugebauer, S. Janiak, A. Vilkanauskyte, T. Erichsen, W. Schuhmann, An electrochemical robotic system for the optimization of amperometric glucose biosensors based on a library of cathodic electrodeposition paints, Macromol. Rapid Commun. 25 (2004) 348–354.
[16] S. Isik, J. Oni, V. Rjabova, S. Neugebauer, W. Schuhmann, Entrapment of metalloporphyrins within an electrodeposition paint layer as a basis for developing of a nitric oxide sensor, Microchim. Acta 148 (2004) 59–64.
[17] A. Vilkanauskyte, T. Erichsen, L. Marcinkeviciene, V. Laurinavicius, W. Schuhmann, Reagentless biosensors based on co-entrapment of a soluble redox polymer and an enzyme within an electrochemically deposited polymer film, Biosens. Bioelectron 17 (2002) 1025–1031.
[18] S. Alpeeva, A. Vilkanauskyte, B. Ngounou, E. Csöregi, I.Y. Sakharov, M. Gonchar, W. Schuhmann, Bi-enzyme alcohol biosensors based on genetically engineered alcohol oxidase and different peroxidases, Microchim. Acta 152 (2005) 21–27.
[19] R.K.R. Charan, F. Turcu, A. Schulte, A.M. Kayasth, W. Schuhmann, Fabrication of a potentiometric/amperometric bifunctional enzyme microbiosensor, Anal. Chem. 15 (2005) 5063–5067.
[20] F. Beck, Fundamental aspects of electrodeposition paint, Prog. Org. Coat 4 (1976) 1.
[21] J. Niemann, Waterborne coatings for the automotive industry, Prog. Org. Coat 21 (1992) 189–203.
[22] W.C. Chen, C.C. Chang, Synthesis and characterization of large diameter acrylic polymer light conduits, J. Mater. Chem. 9 (1999) 2307–2312.
[23] T.P. Wampler, G.A. Bishea, W.J. Simonsick, Recent changes in automotive paint formulation using pyrolysis — gas chromatography/mass spectrometry for identification, J. Anal. Appl. Pyrolysis 40–41 (1997) 79–89.
[24] P.D. Ribeiro, E.W. Alves, O.L.T. Machado, Carboxyl-terminal sequencing: COOH-amino acid activation with DCC or TBTU, Prot. Peptide Letters 6 (1999) 203–208.
[25] I.K. Kang, O.H. Kwon, Y.M. Lee, Preparation and surface characterization of functional group-grafted and heparin-immobilized polyurethanes by plasma glow discharge, Biomaterials 17 (1996) 841–847.
[26] C.H. Chang, Y.M. Sheu, W.P. Hu, L.F. Wang, J.S. Chen, Synthesis and properties of copolymers from 2-hydroxyethyl methacrylate-linked nonsteroidal anti-inflammatory agents with methacrylic acid, J. Polym. Sci., A, Polym. Chem. 36 (1998) 1481–1490.
[27] Z. Cheng-Li, S. Manfred, B. Bertold, W. Harm, H. Wolfgang, Method of coating a shaped mineral articles, US Patent 20010000232.
[28] P.J. Flory, Viscosities of linear polyesters. An exact relation between viscosity and chain length, J. Am. Chem. Soc. 62 (1940) 1057.
[29] T.G. Fox, Influence of diluent and of copolymer composition on the glass temperature of a polymer system, Bull. Am. Phys. Soc. 2 (1956) 1.
[30] T. Erichsen, S. Reiter, W. Märkle, C. Tittel, V. Ryabova, E.M. Bonsen, G. Jung, B. Speiser, W. Schuhmann, Combinatorial microelectrochemistry. Development and evaluation of an electrochemical robotic system, Rev. Sci. Instrum. 76 (2005) 062204.